J Solid State Electrochem (2012) 16:423–428
DOI 10.1007/s10008-011-1387-7

ORIGINAL PAPER

Electrochemical study on lithium iron phosphate/hard carbon lithium-ion batteries

Xiangfei Liao · Ji Yu · Lijun Gao

Received: 12 January 2011 / Revised: 28 February 2011 / Accepted: 3 March 2011 / Published online: 5 April 2011

Abstract The electrochemical performances of lithium iron phosphate ($LiFePO_4$), hard carbon (HC) materials, and a full cell composed of these two materials were studied. Both positive and negative electrode materials and the full cell were characterized by scanning electron microscopy, transmission electron microscopy, charge–discharge tests, and alternating current (a.c.) impedance techniques. Experimental results show that the $LiFePO_4$/HC full cell exhibits a gradually decreased cell voltage, and it is capable of delivering a reversible discharge capacity of 122.1 mAh g^{-1} at 0.2-C rate. At the higher rate of 10 C, the efficiency of the full cell remains almost unchanged from that of 0.2 C. Furthermore, the $LiFePO_4$/HC battery demonstrated a long life of 2,450 cycles with 40% of capacity change at a 10-C high rate. The internal resistance of the full cell is rather low as it is revealed from a.c. impedance measurements. These properties make the $LiFePO_4$/HC battery an attractive option for high rate and long cycle life power applications.

Keywords Lithium iron phosphate · Hard carbon · Lithium-ion battery

X. Liao · J. Yu · L. Gao
Department of Chemistry, Nanchang University, Nanchang 330031 China

L. Gao (✉)
School of Energy, Soochow University, Suzhou 215006 China
e-mail: gaolijun@suda.edu.cn

Introduction

Hybrid electric vehicles (HEVs) play an important role in improving energy efficiency and reducing gas emission. Currently, lithium-ion batteries are being used in HEVs; however, there are many issues to be resolved, such as cost, cycle life, safety, and power density [1, 2]. One of the widely used commercial Li-ion battery cathode materials is $LiCoO_2$ [3]; however, it has some drawbacks such as poor safety and environmental problems which more or less prevent its application in vehicles [4]. The cathode material lithium iron phosphate ($LiFePO_4$) has been considered a promising candidate for HEVs because of its safety, high theoretical capacity of 170 mAh g^{-1}, low cost, and non-toxicity [5, 6]. $LiFePO_4$ has a very flat discharge and charge profile at 3.4 V (vs. Li^+/Li), which makes it adaptable in most electrolytic solutions [7]. In addition, the thermal stability of $LiFePO_4$ is higher than that of other cathode materials such as $LiCoO_2$, $LiNiO_2$, and $LiMn_2O_4$ [8]. The main obstacle for practical application is its inherently low electronic conductivity [9].

For a good electrochemical performance of Li-ion battery, a suitable anode material will be indispensable. Graphite materials such as meso-carbon micro-beads are commonly used in Li-ion batteries as anode because of their high capacity [10, 11]. Hard carbon is another alternative for anode. Sony Corporation has used hard carbon derived from polyfurfuryl alcohol as anode material in its batteries [12]. Compared to graphite, hard carbon has many advantages and also some disadvantages. The advantages include higher capacity, longer life, good rate performance, and lower cost. The disadvantages are mainly concerned with larger irreversible capacity, low density, and hysteresis in the voltage profile [13–15]. In addition, there are some

other carbon-based anode materials such as graphite–coke hybrids, vapor-grown carbon fiber, and low-crystallized carbon [16–18].

The regularly used binder to make Li-ion battery electrodes is polyvinylidene fluoride which is relatively expensive and may affect the performance of batteries as cycles proceed, and the typical solvent is *N*-methyl-2-pyrrolidone which is also relatively expensive and toxic. The objective of this work is to develop an inexpensive Li-ion battery using $LiFePO_4$ as cathode and hard carbon as anode. Both the cathode and anode use environmentally friendly aqueous binder styrene butadiene rubber (SBR) as well as thickening agent carboxymethyl cellulose sodium (CMC). To the best of our knowledge, such a system has not been reported previously in the literature. Electrochemical properties of the $LiFePO_4$/HC Li-ion batteries are characterized by charge and discharge tests, cycle life, and alternating current (a.c.) impedance methods.

Experiment

Preparation of $LiFePO_4$ and hard carbon electrodes

Thin Li-ion coin cells (2025) were composed of hard carbon (BTR, China) as anode, $LiFePO_4$ (Aleees, Taiwan) as cathode, an organic electrolyte, and a polymer separator. The electrolyte was 1.3 M $LiPF_6$ in a mixture (1:3 by mass) of ethylene carbonate and dimethyl carbonate, and the separator was Celgard 2320. The anode electrode assembly was prepared from a slurry of hard carbon with 1 wt.% of conductive carbon (Super-P-Li, Timcal), 2.25% of CMC, and 2.25% of SBR dissolved in de-ionized water. The paste was coated by a doctor-blade process onto a 14-μm thick copper foil current collector. The cathode was prepared by combining 15% of conductive carbon, 2.5% of CMC, 2.5% of SBR, and 80% of $LiFePO_4$ mixed in de-ionized water. The paste was coated on an aluminum foil of 20-μm thickness. After drying at 75 °C in a vacuum for 2–3 h, the laminate electrodes were roll pressed to a thickness of about 28 μm for the cathode and 25 μm for the anode. Electrodes were punched out from the laminates as wafers with 16-mm diameter, then dried under vacuum at 100 °C for 24 h before being assembled into 2025 coin cells in a glove box (Braun) filled with argon gas. The half cell performances of the anode and cathode electrodes were evaluated separately using lithium metal as counter electrode.

Measurements

Profiles of the as-prepared samples were analyzed using scanning electron microscopy (SEM FEI Quanta 200F, 15 kV) and high-resolution transmission electron microscopy (Hitachi H-9000, 150 kV). Particle size distribution of the hard carbon materials was identified by Malvern Mastersizer 2000. Discharge–charge cycle measurements were carried out using a constant current method. An electrochemical workstation IM6ex (Zahner) was employed to measure electrochemical impedance spectroscopy (EIS). During the EIS measurements, frequency was scanned from 100 kHz to 100 mHz and an a.c. voltage oscillation of 5 mV.

A battery test system (Land) was used to measure charge–discharge cycles at room temperature. The cycle lives of the cathode electrode ($LiFePO_4$/Li), anode electrode (HC/Li), and the full cell ($LiFePO_4$/HC) were tested under the mode of constant current followed by constant voltage (CC–CV) for charge and constant current (CC) for discharge. The end of charge voltage (EOCV) and end of discharge voltage (EODV) for $LiFePO_4$/Li and $LiFePO_4$/HC were 3.6 V and 2.2 V, respectively. For the HC/Li half cell, the EODV and EOCV were 0.01 V and 1.8 V, respectively. The CV charge voltage at 3.6 V or 1.8 V was terminated after the current dropped to half value from its initial constant current. The depth of discharge of the cells at these EOCV and EODV can be considered 100% [19]. Before each discharge–charge cycle at high rates (above 1 C), the cells were charged and discharged at 0.2 C for two cycles.

Results and discussion

Figure 1 presents SEM and TEM photographs and particle size distribution of hard carbon material. Spherical-like carbon particles can be observed from the SEM in Fig. 1a. Particle size distribution of the hard carbon material shown in Fig. 1c was rather narrow with an average size of 12 μm in diameter which is consistent with the result of SEM observation. A TEM image is shown in Fig. 1b; the hard carbon has an irregular layered structure, and the distance between each layer is about 0.5 nm. This structure made hard carbon material facile for Li-ion insertion which can result in a high capacity.

Figure 2 shows SEM (a) and TEM (b) photographs of $LiFePO_4$ material. It can be seen from the images that the $LiFePO_4$ particles were rather disbursed, without significant conglomeration. The size of $LiFePO_4$ particles was between 50 and 150 nm in diameter. Carbon fibers can be observed inter-connecting $LiFePO_4$ particles which benefits conductivity improvement of the $LiFePO_4$ electrode.

Figure 3 (a) shows the charge and discharge behavior of the $LiFePO_4$ cathode material at 0.2-C rate in a voltage range of 2.2 V to 3.6 V. The discharge capacity was 157.5 mAh g^{-1}, and the coulombic efficiency was at an outstanding 97.3% which can be attributed to the improved

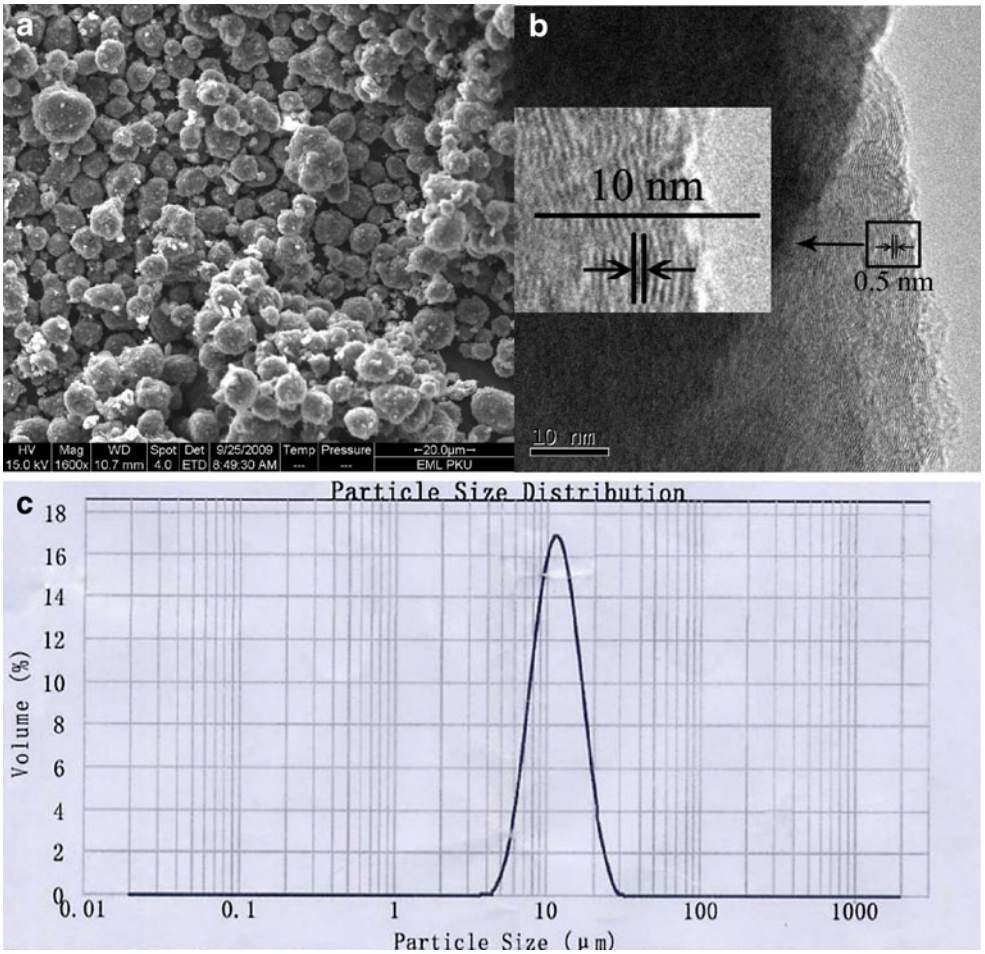

Fig. 1 SEM (**a**), TEM (**b**) photographs and particle size distribution (**c**) of hard carbon material

conductivity of $LiFePO_4$ due to added carbon fibers. The discharge–charge profiles of the first two cycles at 0.2 C for the HC/Li half cell are shown in Fig. 3b. The mechanism that Li-ion inserts in hard carbon material is different from that in graphite material. Though hard carbon is not as fully crystallized as graphite, there is a larger inter-layer space structure in hard carbon. The behavior of Li-ion insertion in hard carbon is determined by surface phenomena at high-energy sites and the filling of micropores [20, 21]. The curve shape of the HC/Li half cell in Fig. 3b is similar to that of the HC anode reported previously [22], and in addition, it has demonstrated better initial coulombic efficiency at 83.0%. Since the surface area of the hard carbon material is quite low at 3.2 $m^2\ g^{-1}$, there is less consumption of surface layer carbon material in reaction with the electrolyte during first charge, and this could be

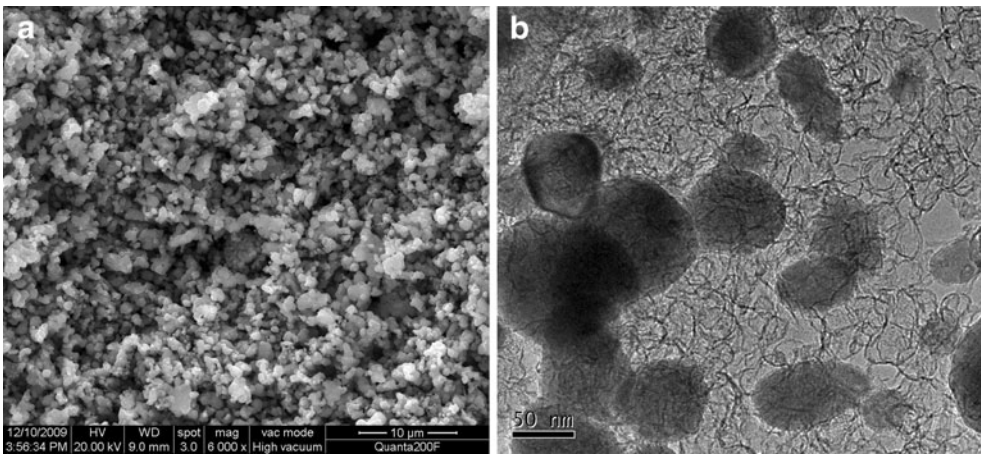

Fig. 2 SEM (**a**) and TEM (**b**) images of $LiFePO_4$ particles

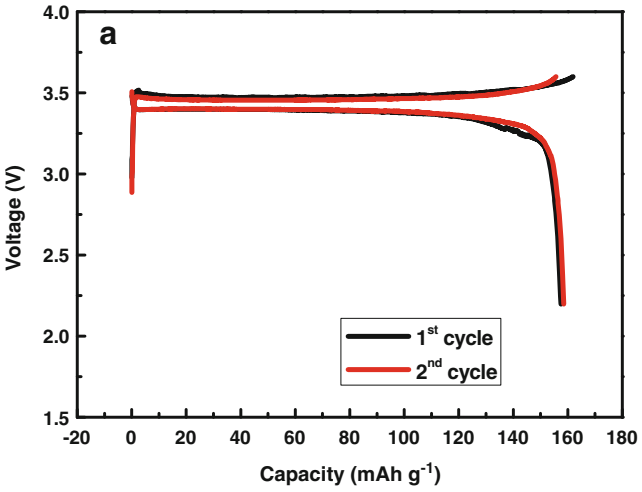

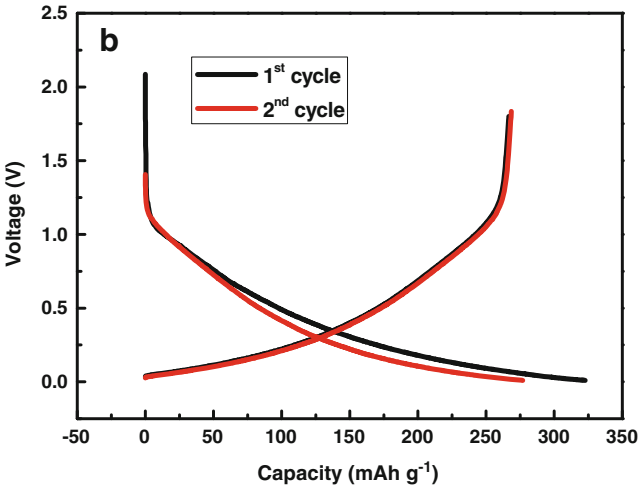

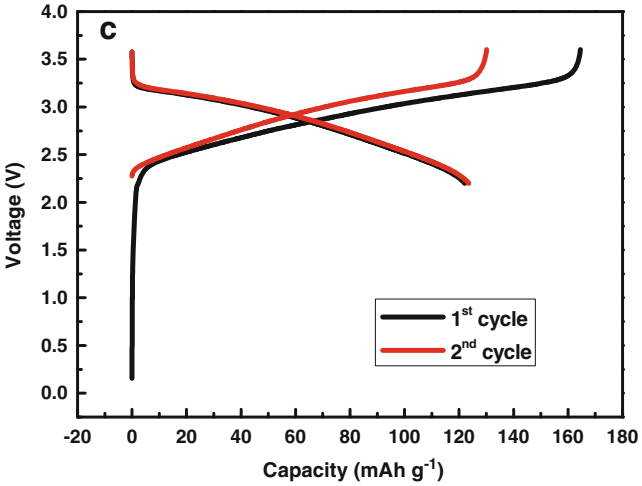

Fig. 3 First two discharge–charge cycles of the half cells of $LiFePO_4$/Li (**a**), HC/Li (**b**), and the full cell $LiFePO_4$/HC (**c**) at 0.2-C rate

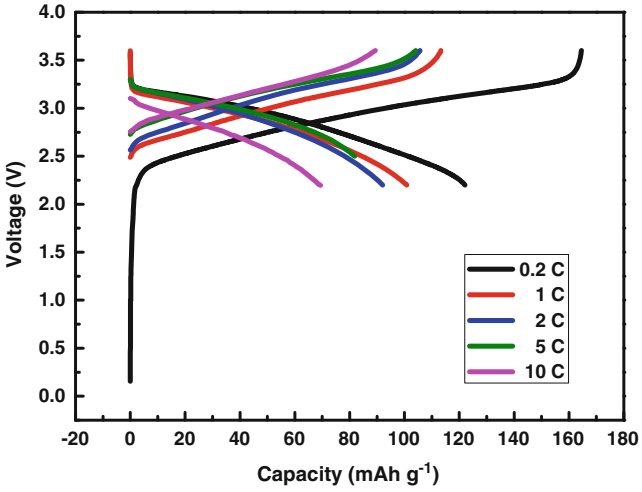

Fig. 4 Charge–discharge profiles of $LiFePO_4$/HC full cells at various rates

one of the reasons for the high efficiency at first SEI film formation. The charge capacity (Li de-intercalation) of 322.7 mAh g^{-1} observed in Fig. 3b for hard carbon can be considered a fair value which is comparable to that of graphite. This is a result of combination behavior from disordered low crystalline structure of hard carbon which diminishes Li-ion capacity and also from the enlarged carbon layer gap of hard carbon which facilitates easier Li-ion insertion/extraction thus contributing to enhanced capacity.

Typical discharge–charge profiles of the $LiFePO_4$/HC full cell at a 0.2-C rate are shown in Fig. 3c; as it is seen,

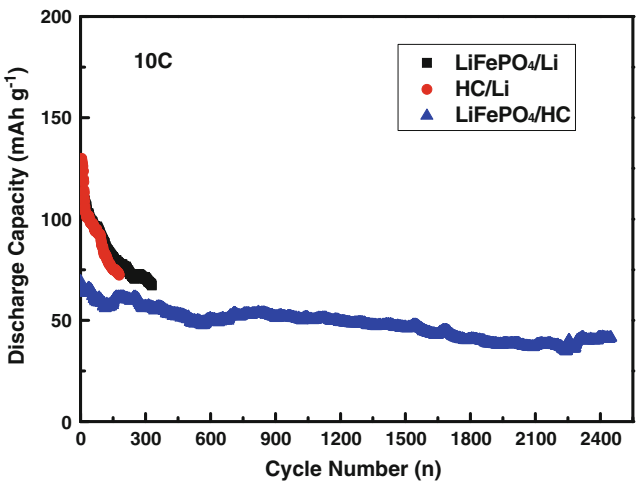

Fig. 5 Cycle performance of half cells ($LiFePO_4$/Li and HC/Li) and full cell ($LiFePO_4$/HC) at 10-C rate

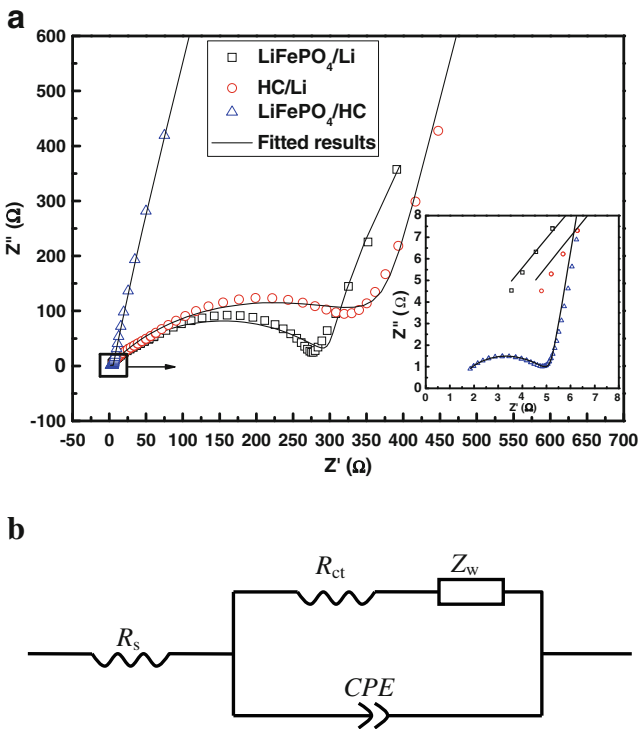

Fig. 6 Impedance spectra of $LiFePO_4$/Li, HC/Li, and $LiFePO_4$/HC cells (**a**) and the equivalent circuit (**b**)

the first charge and discharge capacities are 168 mAh g^{-1} and 121 mAh g^{-1}, respectively, which corresponds to a coulombic efficiency of the first cycle to be 72%. Formation of SEI film at anode is considered to be the main contribution to the loss of efficiency [23, 24]. The shape of the curves is similar to that of the $LiCoO_2$/HC cell reported by Sun [25]; the voltage of the cell gradually decreases which is characteristic of hard carbon material. This is in contrast to the $LiFePO_4$/graphite battery which has a near flat voltage at 3.2 V. A reversible capacity of 123.6 mAh g^{-1} (based on the mass of the $LiFePO_4$ material in the positive electrode) was displayed in the second cycle.

The rate performance of the $LiFePO_4$/HC full cell is shown in Fig. 4. The original specific charge and discharge capacity was achieved at 164.9 and 122.1 mAh g^{-1} at a 0.2-C rate, respectively. At a higher rate of 10 C, the discharge capacity is changed to 69.4 mAh g^{-1}, a 43% drop from that of the 0.2-C rate. However, the coulombic efficiency almost remains unchanged at 71.1% compared to that at 0.2-C rate.

The cycle behavior of the $LiFePO_4$/Li, HC/Li half cells, and the $LiFePO_4$/HC full cell at a 10-C rate is shown in Fig. 5. It can be seen that the cycle life of the full cell was longer than that of each half cell of anode or cathode. After 178 cycles, the discharge capacity of the HC/Li half cell has dropped to 60% of its first discharge capacity. For the $LiFePO_4$ electrode, it took 330 cycles for the discharge capacity to change to 60% from its initial value. The $LiFePO_4$/HC full cell, however, was tested for 2,450 cycles at a 10-C rate, and the discharge capacity was changed from 69.4 mAh g^{-1} to 41.4 mAh g^{-1}. This high rate and long cycle performance demonstrate that the $LiFePO_4$ and hard carbon material combination can result in a promising Li-ion battery.

The EIS results of $LiFePO_4$/Li, HC/Li, and $LiFePO_4$/HC cells in the frequency range from 100 kHz to 100 mHz are shown in Fig. 6a. All Nyquist plots are composed of a semicircle and a straight line in the low-frequency region. The interception at the Z′ axis at high frequency and the semicircle in the middle frequency range are related to the solution resistance (R_s) and the charge transfer resistance (R_{ct}), respectively. The straight line at the low frequency represents the Warburg impedance (Z_w), which is attributed to the diffusion of lithium ions. In the Nyquist plots, the characteristic depressed semi-circles at the high-frequency region can be observed due to the porous nature of powder electrode materials [26–28].

Equivalent circuit of the $LiFePO_4$/Li, HC/Li half cells and $LiFePO_4$/HC full cell is depicted in Fig. 6b. Simulation using ZSimpWin software involving the equivalent circuit model is carried out. The fitting results to the experimental data are quite satisfactory as it is shown in Fig. 6a. The EIS simulation parameters corresponding to the equivalent circuit components are listed in Table 1. The physical meaning of the constant phase element

Table 1 EIS simulation parameters of $LiFePO_4$/Li, HC/Li, and $LiFePO_4$/HC cells

Cells	R_s (Ω cm^2)	CPE (S^n cm^{-2})	n	R_{ct} (Ω cm^2)	W ($S^{0.5}$ cm^{-2})
$LiFePO_4$/Li	3.54	4.11×10^{-5}	0.62	292.2	0.00118
HC/Li	4.57	3.99×10^{-5}	0.62	354.5	0.000233
$LiFePO_4$/HC	1.86	1.67×10^{-5}	0.81	4.99	5.78×10^{-5}

(CPE) represents double layer capacitance with a rough electrode surface. From Fig. 6a and Table 1, it can be seen clearly that the $LiFePO_4$/HC cell displayed a much lower R_{ct} than the half cells of $LiFePO_4$/Li and HC/Li. This phenomenon indicates that the charge transfer reaction at electrode/electrolyte interfaces of the full cell was much easier than that of each half cell, and as a result, the overall battery internal resistance is decreased. The reaction at the Li/electrolyte interface could be an impeding process, which results in a degrading overall performance of the half cells. In addition, the possible formation of microdendrites of lithium metal could be the leading cause of short cycle life half cells at high rates. However, the full cell of $LiFePO_4$/HC has demonstrated satisfactory cycle performance at high rates as it is displayed in Fig. 5.

Conclusions

In this work, the electrochemical performance of the $LiFePO_4$/HC battery was investigated along with $LiFePO_4$ positive and hard carbon negative electrode materials. The hard carbon anode material with an average particle size of 12 μm demonstrated a high initial coulombic efficiency of 83.0% and a charge capacity of 322.7 mAh g^{-1} due to the combined contribution of low crystallization and larger layer gap structure of the hard carbon. The discharge voltage of the $LiFePO_4$/HC cell decreases gradually in contrast to that of the $LiFePO_4$/graphite battery which has a flat voltage. This could be an advantage with convenience in the determination of the state of charge for the $LiFePO_4$/HC battery. Cycle performance tests show the $LiFePO_4$/HC full cell is capable of delivering a long cycle life (2,450 cycles) at a high rate of 10 C. Such a battery could be used in power applications requiring high power and long cycle performance.

Acknowledgments We acknowledge the financial support of this research work from the Natural Science Foundation of **C**hina no. 20663005.

References

1. Terada N, Yanagi T, Arai S, Yoshikawa M, Ohta K, Nakajima N, Yanai A, Arai N (2001) J Power Sources 100:80–92
2. Guerfi A, Duchesne S, Kobayashi Y, Vijh A, Zaghib K (2008) J Power Sources 175:866–873
3. Zaghib K, Striebel K, Guerfi A, Shim J, Armand M, Gauthier M (2004) Electrochim Acta 50:263–270
4. Li J, Suzuki T, Naga K, Ohzawa Y, Nakajima T (2007) Mater Sci Eng B 142:86–92
5. Padhi AK, Nanjundaswamy KS, Goodenough JB (1997) J Electrochem Soc 144:1188–1194
6. Julien CM, Manger A, Ait-Salah A, Massot M, Gendron F, Zaghib K (2007) Ionics 13:395–411
7. Jaiswal A, Horne CR, Chang O, Zhang W, Kong W, Wang E, Chern T, Doeff MM (2009) J Electrochem Soc 156:A1041–A1046
8. Takahashi M, Tobishima S, Takei K, Sakurai Y (2002) Solid State Ionics 148:283–289
9. Song GM, Wu Y, Liu G, Xu Q (2009) J Alloys Compd 487:214–217
10. Forgez C, Do DV, Friedrich G, Morcrette M, Delacourt C (2010) J Power Sources 195:2961–2968
11. Amine K, Liu J, Belharouak I (2005) Electrochem Commun 7:669–673
12. Sekai K, Azuma H, Omaru A, Fujita S, Imoto H, Endo T, Yamaura K, Nishi Y, Mashiko S, Yokogawa M (1993) J Power Sources 43:241–244
13. Buiel E, George AE, Dahn JR (1998) J Electrochem Soc 145:2252–2257
14. Buiel E, Dahn JR (1998) J Electrochem Soc 145:1977–1981
15. Buiel E, Dahn JR (1999) Electrochim Acta 45:121–130
16. Higuchi H, Uenae K, Kawakami A (1997) J Power Sources 68:212–215
17. Abe H, Murai T, Zaghib K (1999) J Power Sources 77:110–115
18. Kida Y, Yanagida K, Funahashi A, Nohma T, Yonezu I (2001) J Power Sources 94:74–77
19. Shim J, Kostecki R, Richardson T, Song X, Striebel KA (2002) J Power Sources 112:222–230
20. Nagao M, Pitteloud C, Kamiyama T, Otomo T, Itoh K, Fukunaga T, Tatsumi K, Kanno R (2006) J Electrochem Soc 153:A914–A919
21. Liu YH, Xue JS, Zheng T, Dahn JR (1996) Carbon 34:193–200
22. Wang Q, Li H, Chen LQ, Huang XJ (2001) Carbon 39:2211–2214
23. Sun H, He XM, Ren JG, Li JJ, Jiang CY, Wan CR (2007) Electrochim Acta 52:4312–4316
24. Guo BK, Shu J, Tang K, Bai Y, Wang ZX, Chen LQ (2008) J Power Sources 177:205–210
25. Sun H, He XM, Li JJ, Ren JG, Jiang CY, Wan CR (2006) Solid State Ionics 177:1331–1334
26. Liu H, Cao Q, Fu LJ, Li C, Wu YP, Wu HQ (2006) Electrochem Commun 8:1553–1557
27. Yin X, Huang K, Liu S, Wang H, Wang H (2010) J Power Sources 195:4308–4312
28. Yang LX, Gao LJ (2009) J Alloys Compd 485:93–97